

# Nonlinear absorption in InN under resonant- and non-resonant excitation

H. Ahn<sup>\*a</sup>, M.-T. Lee<sup>a</sup>, Y.-M. Chang<sup>a</sup>, J. L. Peng<sup>b</sup>, and S. Gwo<sup>c</sup>

<sup>a</sup>Department of Photonics and Institute of Electro-optical Engineering, National Chiao Tung University, Hsinchu 30010, Taiwan, Republic of China; <sup>b</sup>Center for Measurement Standards, Industrial Technology Research Institute, Hsinchu 300, Taiwan, Republic of China; <sup>c</sup>Department of Physics, National Tsing Hua University, Hsinchu 30013, Taiwan, Republic of China

## ABSTRACT

We report the wavelength-dependent nonlinear absorption (NLA) of InN film grown on an *r*-plane sapphire by molecular beam epitaxy technique. In order to understand the nonlinear optical properties of InN, the Z-scan measurement was performed at two different wavelengths, the photon energies of which are near (resonant excitation) and much higher (non-resonant excitation) than the bandgap of InN, respectively. Under non-resonant excitation, band-filling effect leads the dominant saturable absorption, while under resonant excitation, reverse saturable absorption dominates the nonlinear absorption. From the open-aperture Z-scan measurement under resonant excitation, we found that InN exhibits more than one nonlinear absorption process simultaneously. Particularly, under relatively weak resonant excitation, the transformation from saturable absorption to 2PA through the intermediate excitation state absorption was observed as the sample approaches the beam focus. The close-aperture Z-scan signals of InN show valley-peak response, implying that the nonlinear refraction in InN is caused by the self-focusing of the Gaussian laser beam. Using the Z-scan theory, the corresponding nonlinear parameters, such as saturation intensity, 2PA coefficient, and nonlinear refractive index, of InN were estimated.

**Keywords:** nonlinear absorption, indium nitride, z-scan technology

## 1. INTRODUCTION

Indium nitride (InN) with a narrow direct band gap ( $E_g \sim 0.65$  eV) has superior electronic transport properties to other group-III nitrides, which let InN become an attractive material for various applications such as high-frequency electronic devices, near-infrared optoelectronics, and high-efficiency solar cells. Because of its narrow band gap, InN can be easily integrated with an optical fiber laser to realize compact optical system. Recent dramatic increase of information transportation through internet requires switches operating at high rate for future systems development. All-optical switches based on the nonlinear optics may provide solution for faster switches. The bandwidth of optical switch would reach beyond 1 THz unattainable by any electronic switch. In general, all-optical switching technology requires nonlinear materials with large nonlinear refraction, but with relatively small linear absorption. Previous carrier dynamics study on the InN film shows that the InN film excited at wavelength near the band gap has the large optical bleaching and a short carrier lifetime.<sup>1</sup> Especially, the band gap of InN is close to the telecommunication regime, which makes InN an excellent candidate to realize all-optical switch in the information transportation devices. The nonlinear properties of materials can be easily investigated by employing the Z-scan measurement technique.<sup>2</sup> Tsai *et al.* observed saturable absorption (SA) induced nonlinear absorption in InN epitaxial film through the Z-scan measurement at  $\lambda = 800$  nm.<sup>3</sup> For InN film with the absorption edge near 1.9 eV, the fifth-order as well as the third-order nonlinear refractive index was measured and the contribution of the fifth-order nonlinear effect was particularly enhanced for this large band gap InN.<sup>4</sup> At optical telecommunication wavelengths, the third-order nonlinear susceptibility of InN was measured to be at least two orders of magnitude higher than the one of GaN, but is comparable to the values of InGaAsP which is commonly used for communication application.<sup>5</sup> The nonlinear absorption of a thick ( $\sim 1$   $\mu\text{m}$ ) InN film was also reported to be dominated by the saturable absorption and the nonlinear absorption coefficient of  $-1450$  cm/GW and the saturation intensity of  $1.4$  GW/cm<sup>2</sup> were estimated by the Z-scan measurement.<sup>6</sup> However, the estimated values of optical nonlinear parameters for the InN films vary widely and are dependent on the wavelength and the material quality. Moreover, little is known for the details of the nonlinear absorption process at near band gap wavelength including its excitation intensity dependence.

\*hyahn@mail.nctu.edu.tw; phone 886 3 5712121-56369; fax 886 3 5716631

Here, we report the nonlinear optical properties of InN film as measured by Z-scan technique at  $\lambda=800$  and 1550 nm. The photon energies ( $E$ ) of excitation laser beams are larger than  $E_g$  of InN, and the Z-scan signals measured at  $\lambda=800$  and 1550 nm carry the information of NLA under the non-resonant ( $E \gg E_g$ ) and near-resonant ( $E \geq E_g$ ) excitation, respectively. The open aperture (OA) Z-scan signals of the InN film measured at  $\lambda=800$  nm was found to increase near the beam waist, implying NLA is dominated by SA and this SA-dominant NLA behavior persists over a wide intensity range. In contrast, under near-resonant excitation at  $\lambda=1550$  nm, noticeable NLA occurs even at a low intensity and RSA due to multi-photon absorption, especially two-photon absorption (2PA), dominates NLA process. As the intensity increase, 2PA causes the sharp decrease of the transmitted Z-scan signals for InN. The close aperture (CA) Z-scan signals show valley-peak behavior at both wavelengths, indicating self-focusing due to third-order nonlinear refraction.

## 2. EXPERIMENTAL METHOD

### 2.1 Sample preparation

To achieve the transmittance measurement, a thin  $a$ -plane InN epitaxial film was grown by plasma-assisted molecular beam epitaxy (PA-MBE) on an  $r$ -plane  $\{1\bar{1}02\}$  sapphire wafer and a GaN/AlN buffer layer was used between thin InN film and the substrate. Since the linear absorption of InN at 800 nm is large, the thickness of the InN film was kept to be very thin ( $\sim 50$  nm) film to measure the transmitted light at both 800 nm and 1550 nm. The back side of  $r$ -plane sapphire wafer was coated with a Ti layer for efficient and uniform heating during the PA-MBE growth and before transmittance measurement, Ti layer was removed by using diluted HCl solution. The growth direction of the InN film was determined using a  $2\theta$ - $\omega$  x-ray diffraction scan. The photoluminescence spectrum of the InN film was also measured, in which the peak energy locates at  $\sim 0.67$  eV and the bandwidth is narrow ( $< 45$  meV), indicating the high crystalline quality of the film. A separately measured time-resolved reflectance signal displays the ultrafast carrier absorption and recovery processes in InN, confirming the fast lifetime for the realization of all-optical switches.<sup>1</sup>

### 2.2 Experimental set-up

The Z-scan measurements were performed using two lasers with different center wavelengths; a Ti:sapphire laser tunable between 750 and 1080 nm wavelength range with a repetition rate of 82 MHz and a fiber laser which delivers 130 fs laser pulses at 1550 nm with the repetition rate of 70 MHz. Figure 1 illustrates the simple Z-scan measurement setup. During Z-scan measurements, the sample is moved along the optical axis ( $z$ -axis) of the focused laser beam, while the transmittance of the sample is recorded as a function of the  $z$ -position within  $\pm z_0$ , which is given by the Rayleigh length  $z_0$ . The wavelength-dependent Rayleigh diffraction length was calculated to be in the range of 1 – 2.7 mm, which is much longer than the sample thickness. An aperture is placed to prevent some of the light from reaching the detector. In the CA scheme, the aperture causes only the central region of the cone of light to reach the detector. In the OA scheme, the aperture is removed or enlarged to allow all the light to reach the detector and this scheme is used to measure the nonlinear absorption coefficient, while CA z-scan signals are used to elucidate the nonlinear refractive parameters. No noticeable Z-scan signal was detected from the GaN/AlN buffer layer on the sapphire substrate under the same experimental condition, indicating that the Z-scan signals presented in the following are from the thin InN epilayer.

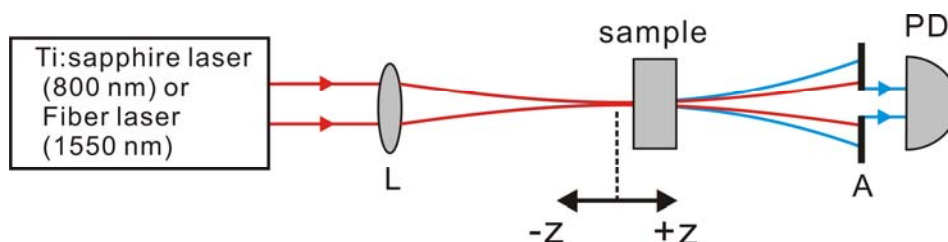


Fig. 1. Simple scheme of Z-scan measurement setup. To provide two different wavelengths near and far above the band gap of InN, a Ti:sapphire laser and a homemade fiber laser was used. L: lens, A: aperture, and PD: photodiode.

### 3. Z-SCAN MEASUREMENT AND THE NONLINEAR ABSORPTION

Z-scan measurement is an effective technique to investigate nonlinear absorption and refraction processes by measuring the transmitted beam energy through OA and CA schemes. Figure 2 shows the power dependent OA Z-scan signals for the InN film measured at  $\lambda=800$  nm. In Fig. 2, the transmitted OA signals increase as the sample approaches the beam waist. This Z-scan feature implies the existence of saturable absorption. At lower laser input intensity, the transmitted signal was too small to get a reasonable signal-to-noise ratio, but similar saturable absorption-induced change of transmittance was observed. [not shown]

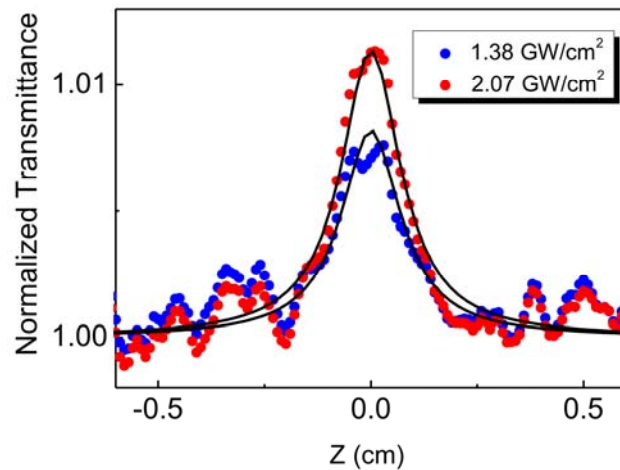


Fig. 2. Normalized open-aperture Z-scan signal at the wavelength of 800 nm measured at two different input intensities. Despite of poor signal-to-noise ratio, the overall Z-scan signal keeps the saturable absorption behavior at even lower input intensity of laser pulse.

Another set of OA Z-scan signals measured at  $\lambda=1550$  nm are shown in Fig. 3. In contrast to the counterpart in Fig. 2, the transmitted signals at  $\lambda=1550$  nm decrease as the sample approaches the beam waist, corresponding to the reverse saturable absorption (RSA). Compared to the ones measured at  $\lambda=800$  nm, the negative change of OA Z-scan signals at  $\lambda=1550$  nm appears at much lower input intensity and is initiated at larger  $-z$  values. Figure 3 also shows that further increase of the input power induces larger negative OA Z-scan signals.

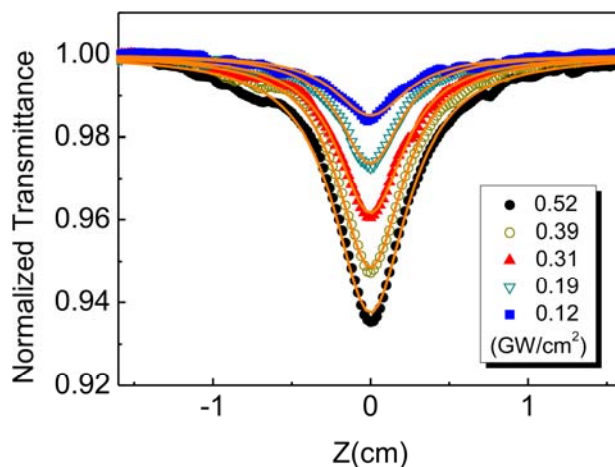


Fig. 3. Input power dependence of normalized open-aperture Z-scan signal measured at the wavelength of 1550 nm. At these input power, only two-photon absorption induced reverse saturable absorption can be observed.

Meanwhile, when the input laser intensity decreases below  $0.12 \text{ GW/cm}^2$ , a new feature shows up. In Fig. 4, the OA signals measured at  $0.03$ ,  $0.06$ , and  $0.12 \text{ GW/cm}^2$  are illustrated. While the one measured at  $0.12 \text{ GW/cm}^2$  shows RSA response, the OA signal measured at  $0.09 \text{ GW/cm}^2$  shows an intermediate NLA response between RSA and SA. A yellow dashed line drawn for eye guiding clearly shows that initially the linear absorption near the band gap saturates the band states and the following NLA evolves to RSA. But this small RSA signal saturates quickly at around  $z \sim -0.15 \text{ cm}$ . As the sample moves toward the focus, the transmission sharply drops again to show a larger and narrower RSA-induced NLA. Increase of the input intensity causes the main negative OA signal to increase, while the contribution of the intermediate RSA response becomes smaller.

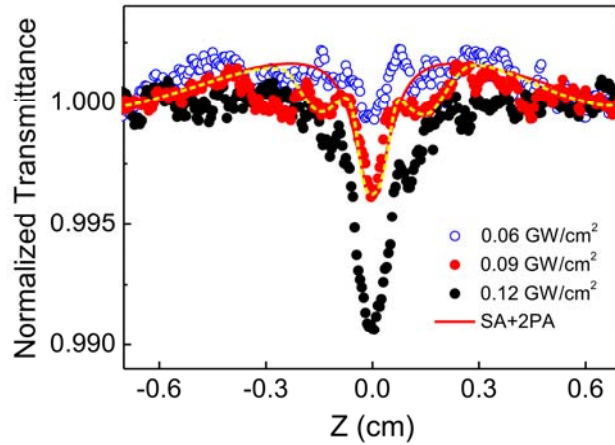


Fig. 4. Normalized open-aperture Z-scan signal measured at the wavelength of  $1550 \text{ nm}$  excited at different input intensity. The red solid line is obtained by considering saturable absorption and two-photon absorption in Eq. (1) and (2).

According to the Z-scan theory, the normalized nonlinear transmittance is related to the sample position  $z$  by<sup>2</sup>

$$T(z) = \frac{1 - \alpha I_0 L_{eff}}{2\sqrt{2} \sqrt{1 + z^2/z_0^2}}, \quad (1)$$

where  $I_0$  is the on-axis peak intensity at the focus,  $L_{eff} = [1 - \exp(-\alpha_0 L)]/\alpha_0$  is the effective interaction length,  $\alpha_0$  is the linear absorption coefficient,  $L$  is the sample length,  $z_0$  is the Rayleigh diffraction length, and the profile of the pulse has been assumed to be Gaussian. Typically, the increase of transmitted OA Z-scan signal near the beam waist corresponds to the SA effect, whereas the decrease of it is due to RSA processes, such as 2PA and excited-state absorption (ESA). 2PA process is a high-order nonlinear optical phenomenon, and thus 2PA occurs at high input intensity. In contrast, ESA is a sequential linear process and thus it can occur at low excitation intensity. Therefore, under certain excitation conditions, both ESA and 2PA may coexist to lead to higher nonlinearities. The observed nonlinear behavior of InN can be described by the modified third-order NLA differential equation as:<sup>7</sup>

$$\frac{dI}{dz} = \alpha(I)I = \left[ \frac{\alpha_0}{1 + I/I_s} - \beta I - \sigma_{ES} \Delta N \right] I \quad (2)$$

where  $I_s$  is the saturation intensity,  $\beta$  is the 2PA coefficient, and  $\sigma_{ES}$  is the ESA cross section. The first term represents the SA process with the saturation intensity  $I_s$  and the second and third terms correspond to RSA processes, 2PA and ESA, respectively. Since the photoexcited carrier density  $\Delta N$  can be calculated by  $\alpha_0 \tau_0 I/h\nu$  and the carrier decay time is much longer than the pulsewidth  $\tau_0$ ,<sup>1</sup> the effective NLA coefficient characterizing RSA takes the form<sup>7</sup>

$$\beta_{eff} = \beta_0 + \sigma_{ES} \alpha_0 \tau_0 / h\nu \quad (3)$$

where the wavelength-dependent  $\alpha_0$  was separately determined by the spectroscopic ellipsometry at 300 K.<sup>8</sup> The solid lines in Fig. 2-4 are the fitted curves using Eq. (1) and (2) including only 2PA and SA. In Fig. 4, SA and 2PA can duplicate the initial increase and the sharp decrease of the OA signal and the discrepancy between experimental data and the solid line shows the existence of an additional RSA process starting at a low intensity, which is ESA. From the fitting parameters, the saturation intensity  $I_s$  at  $\lambda=800$  nm is estimated to be  $\sim 40.37$  GW/cm<sup>2</sup>. Though 2PA process is typically predominant under non-resonant excitation, high photoexcitation can enhance the 2PA cross-section at  $\lambda=1550$  nm and then large negative signals in Fig. 3 is attributed to 2PA process. The dominant contribution of 2PA at  $\lambda=1550$  nm indicates that the incident laser intensity  $I \sim 0.12$  GW/cm<sup>2</sup> exceeds the threshold for 2PA. Meanwhile, the intermediate NLA observed in Fig. 4 indicates that carriers excited to near the bottom of the conduction band through the interband absorption can be re-excited to even higher band states through ESA. Similar switchover between ESA and 2PA has been observed in axial-bonding type hybrid porphyrin arrays.<sup>9</sup>

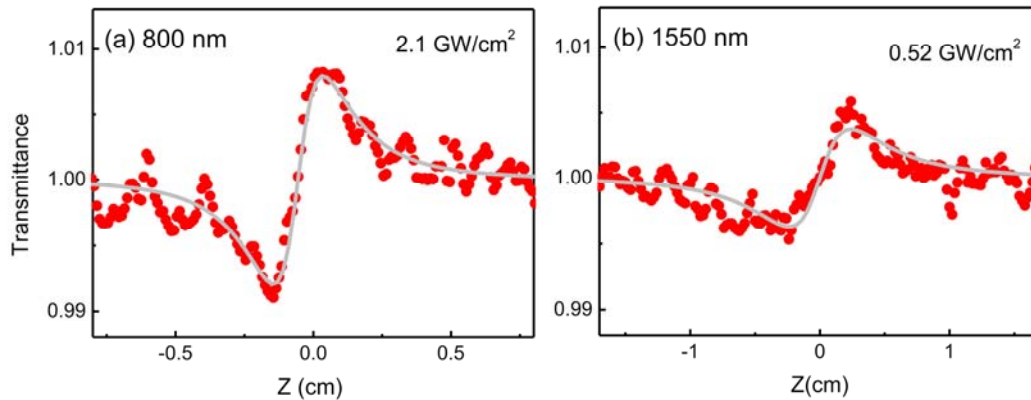


Fig. 5 The closed-aperture Z-scan signals of the InN film measured at 800 nm and 1550 nm, respectively. The transmittances of both wavelengths show the valley-peak response, corresponding to self-focusing.

High intensity excitation also induces the change in the refractive index, which can be described as  $n=n_0+n_2I$  with the nonlinear refractive index  $n_2$ . The measurement of the nonlinear index of bulk samples is often achieved with the CA Z-scan measurement. In Fig. 5, the transmitted CA profiles of InN measured at  $\lambda = 800$  nm and 1550 nm exhibit similar valley-peak responses, indicating the self-focusing. The nonlinear refractive index  $n_2$  was found to be  $5.9 \times 10^{-11}$  and  $1.9 \times 10^{-10}$  for  $\lambda = 800$  nm and 1550 nm, respectively. In a Kerr-like media, the refractive index  $n(r)$  has the same radial profile as the laser  $I(r)$ , thus providing  $\Delta T_{p-v} \sim 1.7z_0$ , where  $\Delta T_{p-v}$  is the distance between the valley and the peak transmittance.<sup>2</sup> However, if there is the thermal lens effect,  $n(r)$  is typically wider than  $I(r)$  due to the radial thermal diffusion and  $\Delta T_{p-v}$  becomes much larger than  $1.7z_0$ . From the CA Z-scan curves, we obtained  $\Delta T_{p-v} \sim 1.75z_0$  at both  $\lambda = 800$  nm and 1550 nm, implying that the observed self-focusing in InN is due to the electronically-induced nonlinear refraction index, not due to the thermal-lens effect.

#### 4. SUMMARY

In summary, nonlinear absorption coefficient and nonlinear refractive index of InN were measured by using the femtosecond Z-scan technique. For near-resonant excitation with  $\lambda = 1550$  nm laser pulses, an intermediate NLA process was observed, which includes saturable absorption, excited-state absorption, and two-photon absorption. In particular, it was the first time to observe the excited-state absorption in the InN film. As the input intensity increases, the multi-photon absorption dominates the nonlinear absorption in the InN film. At  $\lambda = 800$  nm, the nonlinear absorption requires much higher input intensity to be excited and the nonlinear absorption process is dominated by the absorption saturation of band states. The nonlinear refractive index of InN at  $\lambda = 1550$  nm is found to be larger than the value at  $\lambda = 800$  nm and this large nonlinearity would enable InN to be an excellent and sensitive nonlinear material for devices with small size and operating with low input pump power at near-infrared spectral range.

## ACKNOWLEDGEMENTS

This work was supported by the National Science Council (Grant No. NSC-101-2112-M-009-MY3 and the Science Vanguard Research Program, Grant No. NSC-101-2628-M-007-006) in Taiwan.

## REFERENCES

- [1] H. Ahn, C.-C. Yu, P. Yu, J. Tang, Y.-L. Hong, and S. Gwo, "Carrier dynamics in InN nanorod arrays," *Opt. Exp.* (2012).
- [2] M. Sheik-Bahae, A. A. Said, T. H. Wei, D. J. Hagan, and E. W. Van Stryland, "Sensitive measurement of optical nonlinearities using a single beam," *IEEE J. Quantum Electron.* **26**, 760 (1990).
- [3] T.-R. Tsai, T.-H. Wu, J.-C. Liao, T.-H. Wei, H.-P. Chiang, J.-S. Hwang, D.-P. Tsai, and Y.-F. Chen, "Characterization of nonlinear absorption of InN epitaxial films with femtosecond pulsed transmission Z-scan measurements," *J. Appl. Phys.* **105**, 066101 (2009).
- [4] Z. Q. Zhang, W. Q. He, C. M. Gu, W. Z. Shen, H. Ogawa, and Q. X. Guo, "Determination of the third- and fifth-order nonlinear refractive indices in InN thin films," *Appl. Phys. Lett.* **91**, 221902 (2007).
- [5] F. B. Naranjo, M. Gonzalez-Herraez, H. Fernandez, J. Solis, and E. Monroy, "Third order nonlinear susceptibility of InN at near band-gap wavelengths," *Appl. Phys. Lett.* **90**, 091903 (2007).
- [6] F. B. Naranjo, P. K. Kandaswamy, S. Valdueza-Felip, V. Calvo, M. Gonzalez-Herraez, S. Martin-Lopez, P. Corredera, J. A. Mendez, G. R. Mutta, B. Lacroix, P. Ruterana, and E. Monroy, "Nonlinear absorption of InN/InGaN multi-quantum-well structures at optical telecommunication wavelengths," *Appl. Phys. Lett.* **98**, 031902 (2011).
- [7] Y. J. Ma, J. I. Oh, D. Q. Zheng, W. A. Su, and W. Z. Shen, "Tunable nonlinear absorption of hydrogenated nanocrystalline silicon," *Opt. Lett.* **36**, 3431 (2011).
- [8] H. Ahn, C.-H. Chen, C.-L. Wu, and S. Gwo, "Spectroscopic ellipsometry study of wurtzite InN epitaxial films on Si.111. with varied carrier concentrations," *Appl. Phys. Lett.* **86**, 201905 (2005).
- [9] P. P. Kiran, D. R. Reddy, A. K. Dharmadhikari, B. G. Maiya, G. R. Kumar, and D. N. Rao, "Contribution of two-photon and excited state absorption in 'axia-bonding' type hybrid porphyrin arrays under resonant electronic excitation," *Chem. Phys. Lett.* **418**, 442 (2006).